Available online at www.sciencedirect.com
ScienceDirect
Polymer 47 (2006) 6765–6772
polymer
www.elsevier.com/locate/polymer

Hyperbranched polyimides crosslinked with ethylene glycol diglycidyl ether: Glass transition dynamics and permeability

V.A. Bershtein [a,*], L.M. Egorova [a], P.N. Yakushev [a], P. Sysel [b], R. Hobzova [b], J. Kotek [b], P. Pissis [c], S. Kripotou [c], P. Maroulas [c]

[a] *Ioffe Physico-Technical Institute of the Russian Academy of Sciences, Department of Solid State Physics, 26 Politechnicheskaya str. 194021 St. Petersburg, Russia*
[b] *Department of Polymers, Institute of Chemical Technology, 5 Technicka, 16628 Prague 6, Czech Republic*
[c] *Department of Physics, National Technical University of Athens, Zografou Campus, 15780 Athens, Greece*

Received 9 June 2006; received in revised form 21 July 2006; accepted 22 July 2006
Available online 10 August 2006

Abstract

A series of amine-terminated hyperbranched polyimides (HBPIs), based on 2,4,6-triaminopyrimidine and 4,4′-oxydiphthalic anhydride and differently crosslinked (by 5–100%) with ethylene glycol diglycidyl ether (EGDE), were prepared. Combined characterization of dynamics in the films obtained, over the temperature range between 20 and 300 °C, was performed using differential scanning calorimetry, thermally stimulated depolarization currents, dynamic mechanical analysis, and laser-interferometric creep rate spectroscopy techniques. For the first time, a peculiar glass transition dynamics was revealed in the HBPIs including two- or three-stage transition; its manifestation over the extremely broad temperature range extending from about 100 to 280 °C; quite different displaying of the glass transition depending on the measuring technique used, and decreasing glass transition temperatures with an increase in crosslinking density. These results could be treated in terms of separate dynamics of exterior and interior domains in HBPI molecular nanoglobules and increasing free volume in HBPIs, in particular due to crosslinking with EGDE. Preliminary estimation of transport parameters for air gases confirmed the good prospects for attaining considerably increased permeability and selectivity in the crosslinked HBPI films studied as compared with those for linear polyimide.

Keywords: Polymer physics; Hyperbranched polyimides; Linear polyimide

1. Introduction

Polymers with highly branched, globular macromolecular structures have attracted increasing attention in recent years because they are expected to have unique properties when compared to their linear analogues. Thus, various dendrimers including aromatic polyimides [1], as perfect and monodisperse macromolecules, are characterized with the highly branched, well-defined structure and a large number of terminal functional groups. Their synthesis, however, involves multi-step procedures leading to high cost and difficulties in large-scale preparation.

Hyperbranched (HB) polymers attracted much interest as well from both fundamental and practical viewpoints [2,3]. Unlike dendrimers, HB polymers do not have the well-defined architecture but can be simply prepared, e.g., from bifunctional and trifunctional monomers. Their globular molecules are generally composed of three types of molecular fragments: dendritic and linear units, and many terminal functional groups. These polymers are thought to have similar properties to dendrimers, to some extent, and can be used to replace dendrimers in most cases.

It is well known that linear polyimides (PIs) are outstanding materials with excellent thermal, mechanical and other properties. Amongst their numerous applications, PIs have also been identified as the high-performance membrane materials for separation of gas mixtures [4]. They show high selectivities

* Corresponding author. Tel.: +7 812 2927172; fax: +7 812 2971017.
E-mail address: vbersht@polmater.ioffe.ru (V.A. Bershtein).

0032-3861/$ - see front matter © 2006 Published by Elsevier Ltd.
doi:10.1016/j.polymer.2006.07.056

but their permeability is insufficient in many cases [4–7], due to dense packing of rather rigid polymer chains.

The permeability of gases through a polymeric membrane depends both on diffusivity and solubility of the permeating species in that polymer. The diffusion coefficient is strongly influenced by free volume, molecular dynamics and polymer structure. From the point of view of a controllable free volume, HB polymers are expected to be a very attractive candidate for preparing membranes with appropriate transport characteristics. In fact, according to results of computer simulations, many open and accessible cavities (free volume holes with typically several angstroms in size) may be expected in rigid HB polymers [8]. Such cavities are mainly formed at the periphery regions of neighboring branches of globular HB macromolecules and may presumably function as additional pathways for the transportation of gas molecules.

In recent years, increasing attention has been paid to synthesis of different types of hyperbranched polyimides (HBPIs) [6,9–36] including also some HBPI-based systems, e.g., such as ethylene glycol diglycidyl ether- [6,9,36] or terephthaldehyde-crosslinked HBPIs [6,9]; hyperbranched poly(imide silsesquioxane) [23]; triazine-containing HBPIs [26]; HBPI-silica hybrids [25,27] or star-like poly(ethylene oxide)s using HBPI as a central core [32]. Up to now, there are already some results indicating the good prospects for applying these polymeric systems as photosensitive materials [18,19,22,30,31] or high-performance membranes [6,23,25–27,36]. Thus, the first publications in fact provide support to the above assumptions on the increased gas permeability: two types of HBPIs, amine-terminated and anhydride-terminated, were obtained and successfully tested as membranes for separation of gas mixtures [6,9,36]; much higher gas permeability coefficients were observed for amine-terminated HBPIs than for the corresponding anhydride-terminated ones.

However, the synthesis of HBPIs from trifunctional monomers requires special and controlled reaction conditions to avoid formation of insoluble gel before films are formed [6,23,33,34]. Besides, highly branched polymer structures have poor mechanical properties because of the formation of globular macromolecules, i.e. due to the lack of chain entanglement [8].

In view of the complicated molecular structure of HBPI systems, it is natural to expect manifestation of their peculiar, complicated molecular dynamics; this problem is, obviously, of both physical and applied interest. However, the studies mentioned above do not provide sufficient information on this topic.

The present work[1] was aimed at studying the glass transition dynamics, using four complementary techniques, and permeability control in a series of amine-terminated HBPIs based on 4,4′-oxydiphthalic anhydride (ODPA) and 2,4,6-triaminopyrimidine (TAP), crosslinked to different extent with ethylene glycol diglycidyl ether (EGDE), due to reaction between amine and epoxy groups. TAP was used before for synthesis of HBPIs in three works [28,35,36]. Of importance, the difficulties, associated with the undesirable formation of three-dimensional product (gel) in solution, could be surmounted in this case owing to different reactivities of amino groups TAP in position 2 and positions 4 and 6 (Fig. 1). This difference was first presumed in Ref. [35], and then supported experimentally by performing model reactions with low-molecular weight compounds [36]. Besides, it was supposed that crosslinking HBPI molecular nanoglobules with EGDE will result in improvement of the mechanical stability and formation of self-standing HBPI films.

[1] This work was presented at the 5th International Symposium on Molecular Mobility and Order in Polymeric Systems (St. Petersburg, 2005).

2. Experimental section

2.1. Materials

Synthesis of the HBPIs studied was described in detail elsewhere [36]. First, a hyperbranched poly(amic acid) (HBPAA) end-capped with amino groups, as HBPI precursor, was prepared from ODPA (Chriscev, USA) and TAP (Aldrich, Czech Republic) taken in a molar ratio of 1:1, and using 1-methyl-2-pyrrolidone (NMP, Merck, Czech Republic) as solvent. Then, the proper amount of the crosslinking agent, EGDE (Aldrich), calculated to reach the required crosslinking level (crosslinking density, c.d.), was added to a 15 wt% solution of HBPAA. The mixtures of HBPAA and EGDE in NMP were spread onto a glass substrate. It should be noted that the real crosslinking densities may differ, to some extent, from the theoretical, calculated values. It may be possible since accessibility of the ''internal'' amine groups for EGDE may be lower in comparison with those close to the globule surface. Such groups may present, obviously, due to some folding the peripheral chains back into the interior of the globules and for other reasons. In fact, the calculated crosslinking density is the ''maximally attainable one'' for the given composition.

Transparent films of crosslinked HBPIs with 0.06 ± 0.03 mm thickness were obtained after simultaneous thermal imidization/crosslinking procedure performed under the following curing conditions: 16 h at 60 °C, 1 h at 100 °C, 1 h at 150 °C, 2 h at 200 °C and, finally, 1 h at 230 °C. The final treatment temperature was a compromise between the full imidization and degradation of the films. Anyway, no signals corresponding to amide groups were found in the IR spectra of the final products. Besides, the IR spectra also confirmed that crosslinking reaction really occurred. Compositions with calculated c.d. = 0, 5, 10, 15, 20, 25, 30, 35, 40, 50, 75 and 100% were obtained and studied. Fig. 1 shows schematically the anticipated structures of amine-terminated HBPIs before and after their crosslinking (see discussion below).

2.2. Characterization

Differential scanning calorimetry (DSC) curves were measured using the Perkin–Elmer DSC-2 apparatus that was calibrated with water (273.1 K), cyclohexane (279.6 K), and indium (429.8 K); heat capacity scale was calibrated using

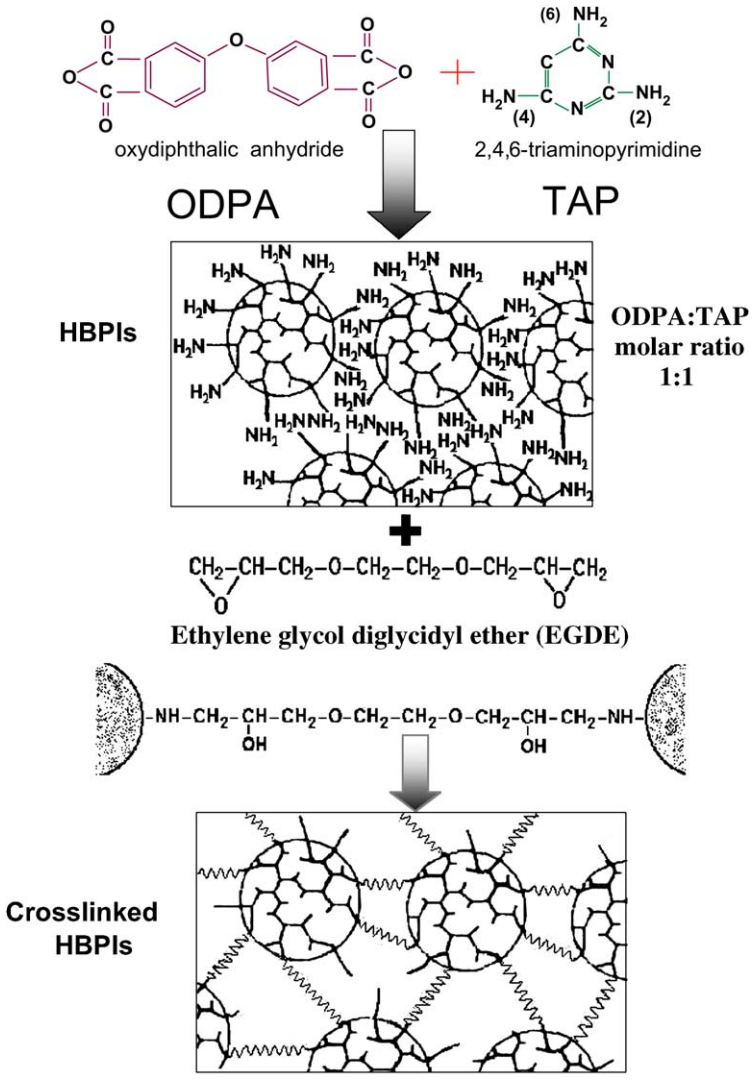

Fig. 1. A simplified scheme of the anticipated structures of HBPIs studied before and after crosslinking with EGDE.

sapphire. The experiments were carried out under nitrogen atmosphere. Three heating scans were performed at a rate of 20 K min^{-1}, the first from −50 to 227 °C, and the second and third from 20 to 260 °C, separated by rapid cooling to 20 °C at a rate of 320 K min^{-1}. The DSC curves of scans II and III practically coincided. Glass transition in HBPIs was characterized by the glass transition temperature T_g recorded at the half-height of the heat capacity step ΔC_P, the onset, T_g', and completion, T_g'', temperatures of the ΔC_P step (transition range), and the value of the ΔC_P step. The equivalent frequency of DSC experiments is equal to $\sim 10^{-2}$ Hz.

Thermally stimulated depolarization current (TSDC) measurements [37] were carried out using a Keithley 617 electrometer in combination with a Novocontrol Quatro cryosystem and a Novocontrol sample cell for TSDC measurements. The experiments were carried out on circular films with 14 mm in diameter over the temperature range from 20 to 230 °C. The film sample was inserted between the brass plates of a capacitor, heated to polarization temperature T_P, and polarized by the application of electric field $E_P = 6$ kV cm^{-1} for time $t_P = 5$ min. The polarization temperature for each sample was chosen properly (T_P close to T_g) to separate glass transition peak from a steep increase of current at higher temperatures associated with conductivity effects [37]. Then, with the electric field still applied, the sample was cooled to 20 °C, short-circuited and reheated; the cooling and heating rates were 6 K min^{-1} and 3 K min^{-1}, respectively. A discharge current was measured as a function of temperature. The equivalent frequency of TSDC measurements spans from 10^{-4} to 10^{-3} Hz [37].

Dynamic mechanical analysis (DMA) was performed with a DMA DX 04T apparatus (RMI, Bohdanec, Czech Republic) at 1 Hz, in the temperature range from 20 to 300 °C, at the heating rate of 3 K min^{-1}.

Laser-interferometric creep rate spectroscopy (CRS) technique using Doppler effect [38–40] was used in this work only for comparing a crosslinked HBPI with a linear PI; insufficient mechanical strength of non- or slightly crosslinked HBPIs prevented detailed studies by this method. The time evolution of sample deformation was registered as a sequence

of beats in an interferogram whose beat frequency ν yielded a creep rate

$$\dot{\varepsilon} = \frac{\lambda \nu}{2I_0} \quad (1)$$

where $\lambda = 630$ nm is the laser wavelength, and I_0 is an initial length of a sample. Samples with about 0.05×8 mm^2 cross-section and 10 mm "working" length were used in these experiments. The creep rate spectra were measured at tensile stress of 1 MPa or 8 MPa, over the temperature range from 20 to 250 °C, at the heating rate of 1 K min^{-1}. The equivalent frequency of the CRS experiments spans from about 10^{-3} to 10^{-2} Hz.

Preliminary gas permeability measurements were performed for some of the HBPIs studied. The permeability coefficients for N_2, O_2 and CO_2 were determined by the integral permeation method. The homemade setup consists of two identical, sample and reference, cells divided by a polymeric membrane into two compartments. Sample gas was introduced into the lower compartment and penetrated through the membrane to the upper compartment filled with hydrogen. The change of the thermal conductivity of the gas mixture in the sample cell was measured versus the initial thermal conductivity of hydrogen in the reference cell.

3. Results and discussion

Fig. 2 shows typical DSC curves obtained over the temperature range from −50 to 260 °C for the HBPI before and after crosslinking. The endotherms with maxima at about 120 °C in the first scan are due to water desorption. They indicate much higher water content in HBPIs as compared with linear PIs. The DSC curves, obtained at the second and subsequent scans, show unusual, two-stage and intense glass transition in the HBPIs that covers very broad temperature range extending from ca. 100 to 200–250 °C, unlike normally weak, one-stage glass transition with about 20 °C width in linear PIs [41]. Fig. 2 shows also decreasing of both glass transition temperatures, T_{g1} and T_{g2}, as well as narrowing glass transition 1 and broadening of glass transition 2 as a result of crosslinking. Fig. 3 shows the DSC curves for several HBPIs with different crosslinking degrees. One can see that the same two-stage transition is observed in all cases, irrespective of crosslinking density. Besides transition temperatures, heat capacity steps are also designated.

Fig. 4 summarizes the DSC data, glass transition temperatures and heat capacity step values, obtained for all HBPI samples studied, as a function of crosslinking density. Somewhat non-monotonous decreasing of the glass transition temperatures is observed at the early stages of crosslinking, up to c.d. = 35–40%; then, at higher crosslinking densities, these temperatures remain practically constant (Fig. 4a). As a result, T_{g1} and T_{g2} decreased by 35 and 55 °C, respectively, with crosslinking. Interestingly, the intensity (as estimated by ΔC_P) of the glass transition 1 did not practically change with crosslinking, whereas ΔC_P increased twice for the glass transition 2 (Fig. 4b).

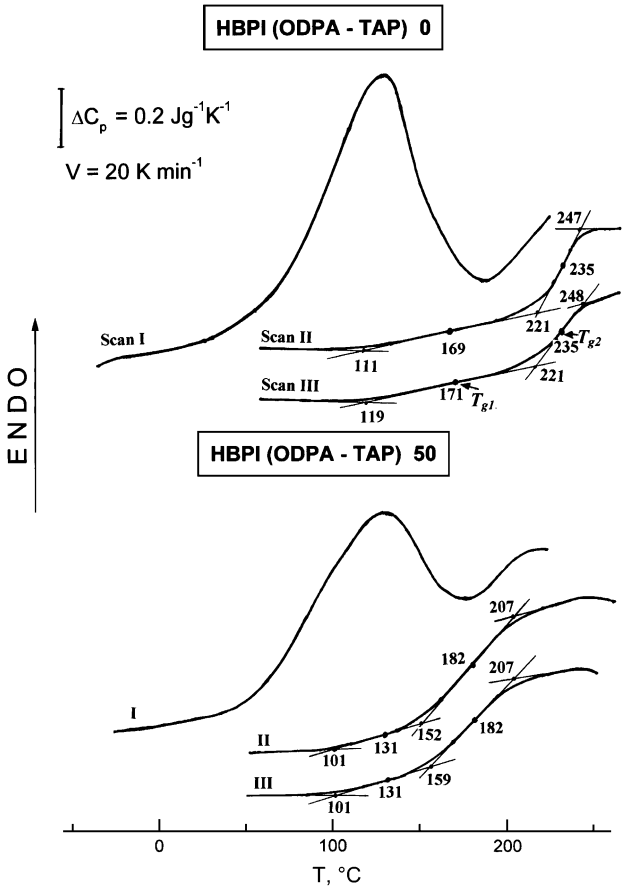

Fig. 2. Typical DSC curves of HBPIs without (upper curves) and after crosslinking with EGDE (by 50%, lower curves), obtained at heating from −50 to 227 °C (scan I), and at repeated scans II and III to 260 °C, after cooling at the rate of 320 K min^{-1}. Heating rate was 20 K min^{-1}. Characteristic glass transition temperatures (see Section 2) are indicated in the plot.

The other peculiarity of HBPI dynamics is the different pattern of glass transition depending on the technique used. Unlike the distinct two-stage glass transition found by DSC, the other techniques revealed either one-stage (TSDC and DMA measurements) or three-stage glass transition (CRS technique) in these polymeric systems.

Fig. 5 shows TSDC thermograms obtained in the temperature region of the glass transition for several HBPIs, differently crosslinked or non-crosslinked. The polarization temperature was chosen properly for each sample to separate the glass transition peak from a steep rise in discharge current I at higher temperatures, which was associated with a sharp increasing conductivity. In all cases one can see only a single, broad TSDC glass transition peak, extending from about 100 to 210 °C for non-crosslinked HBPI, but from 70–90 to 200 °C (c.d. = 10%), 160 °C (c.d. = 20%), or 130–140 °C (c.d. = 35–100%) for crosslinked HBPIs. The maximum of the TSDC peak (T_g value [37]) decreased with crosslinking from ~180 to 110 °C. And, again, as in the DSC measurements, approximately constant T_g value was observed for the samples with c.d. = 35, 75 or 100%. However, TSDC thermograms show only a peak corresponding approximately to the lower-temperature DSC glass transition 1 (compare Figs. 3 and 5).

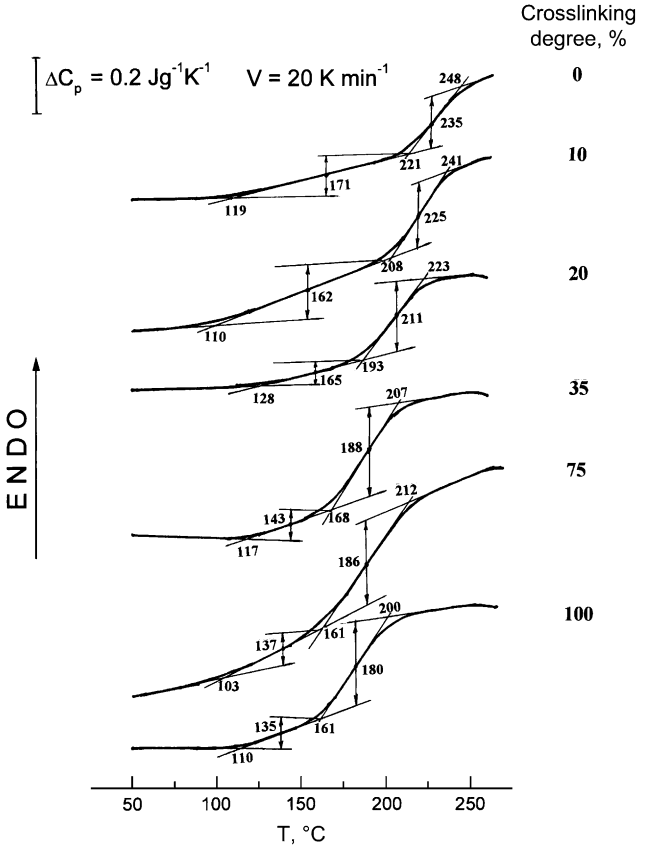

Fig. 3. DSC curves of several HBPIs with different crosslinking degrees, obtained at heating from 20 to 260 °C. Scan III after cooling from 227 °C with the rate of 320 K min^{-1}. Heating rate was 20 K min^{-1}. Characteristic glass transition temperatures and heat capacity steps are indicated.

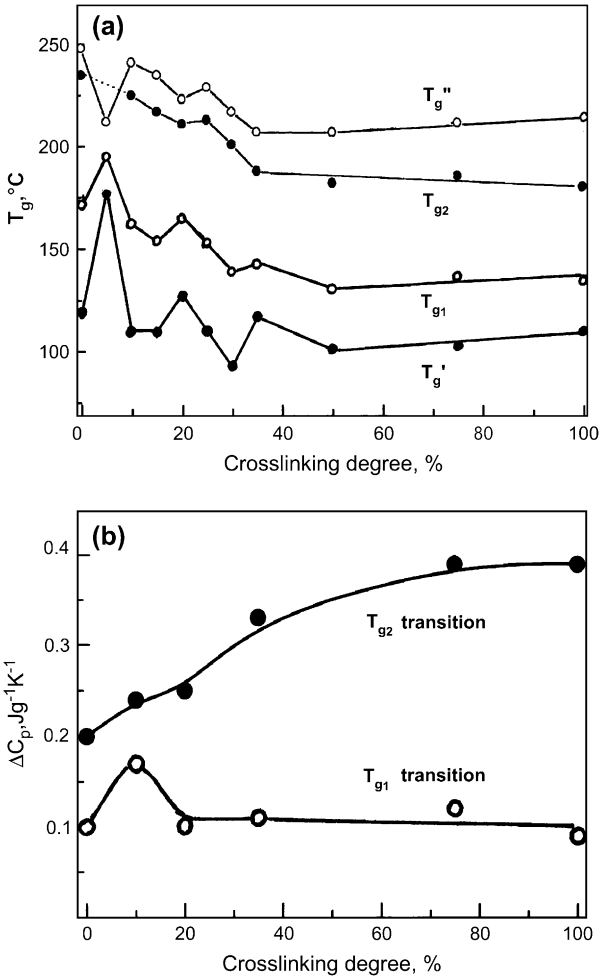

Fig. 4. DSC data: (a) glass transition temperatures and (b) heat capacity step versus crosslinking degree in the HBPIs studied.

Fig. 6 shows two typical DMA spectra of the HBPIs studied. Again, only one glass transition peak is observed in this case, but it starts from about 200 °C, i.e., it corresponds, obviously, rather to DSC glass transition 2 (compare Figs. 3 and 6).

Finally, Fig. 7 shows a special dynamic behavior of HBPI in the CRS measurements. It should be noted that some improvement of mechanical stability, caused by crosslinking HBPI nanoglobules, was attained that allowed us performing some CRS experiments; however, this effect was insufficient for slightly crosslinked HBPIs. In Fig. 7, the creep rate spectrum of crosslinked HBPI (c.d. = 35%) is compared with the spectrum of linear PI prepared from 4,4′-oxydiphthalic anhydride and oxydianiline (ODPA–ODA). The spectrum of linear PI, measured at temperatures below $T_g \approx 280$ °C, exhibits, as usually, β-relaxation peak at 50–100 °C and some "intermediate" relaxations at $T_i \approx 150$, 200 and 230 °C where $T_\beta < T_i < T_g$. In contrast, the creep rate spectrum of HBPI is quite different and characterized by two features, viz., (1) the absence of β-peak despite even using much higher tensile stress, and (2) three-step manifestation of glass transition dynamics. The first, smallest "step" at ca. 130 °C corresponds practically to T_{g1} (DSC). The third step at ca. 170 °C, broken off due to fracture of the sample, is close to T_{g2} (DSC). Besides, an "intermediate" step at ~150 °C may be also seen in the spectrum.

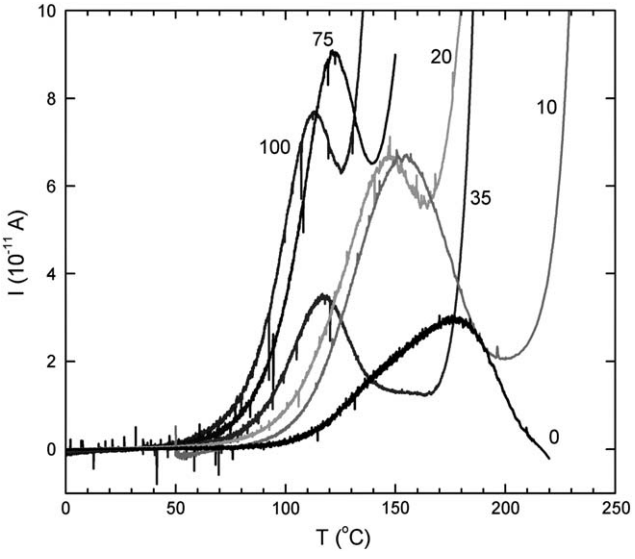

Fig. 5. TSDC spectra of several HBPIs with indicated crosslinking degrees (%) in the temperature region of glass transition. A steep increase of current at higher temperatures was associated with conductivity effects.

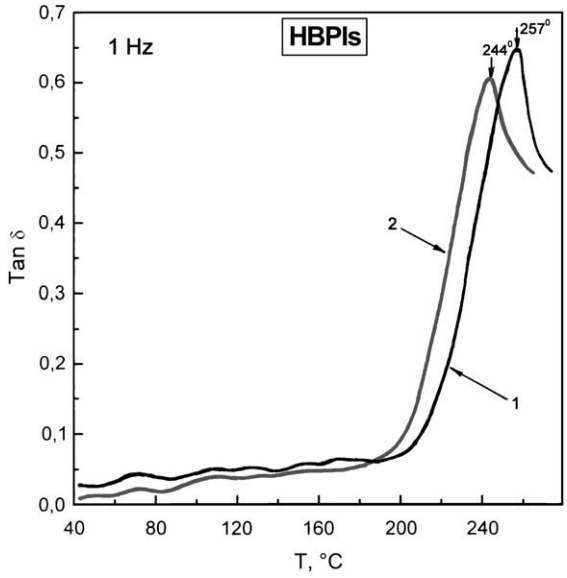

Fig. 6. Typical mechanical loss (DMA) spectra obtained at 1 Hz for the crosslinked HBPIs with c.d. = 15% (1) and 25% (2).

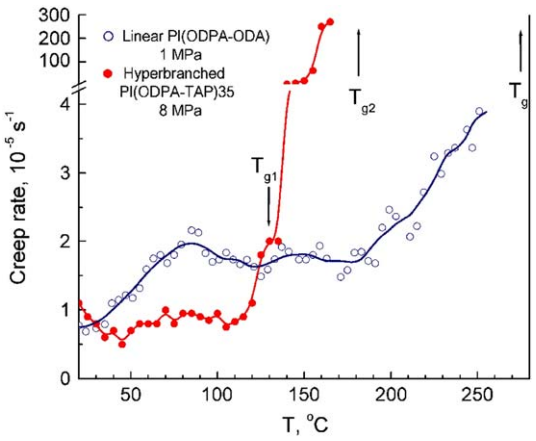

Fig. 7. Comparative creep rate spectra obtained for linear ODPA–ODA polyimide and EGDE-crosslinked hyperbranched ODPA–TAP polyimide (c.d. = 35%). T_g, T_{g1} and T_{g2} arrows correspond to glass transition temperatures as estimated by DSC in these linear PI and HBPI, respectively.

Fig. 8 summarizes the T_g values obtained for all HBPIs studied as a function of the degree of crosslinking with EGDE, measured by three different techniques. In all cases, a common tendency is observed, viz., T_g of the films decreases with the level of crosslinking, being nearly constant for the samples with c.d. = 35–100%. Besides, rather large differences, up to ~100 °C, are observed in the T_g values found for each composition by the different techniques.

The results reported above are unusual and indicate a special glass transition dynamics in HBPIs. Actually, crosslinking renders polymeric materials normally more rigid, and their T_g typically increases with crosslinking density. The difference in T_g values, as measured for a HBPI film by different techniques, may partly be associated with different time (frequency) experimental conditions. Thus, that may explain the difference between T_{g1} (DSC) and T_g (TSDC)

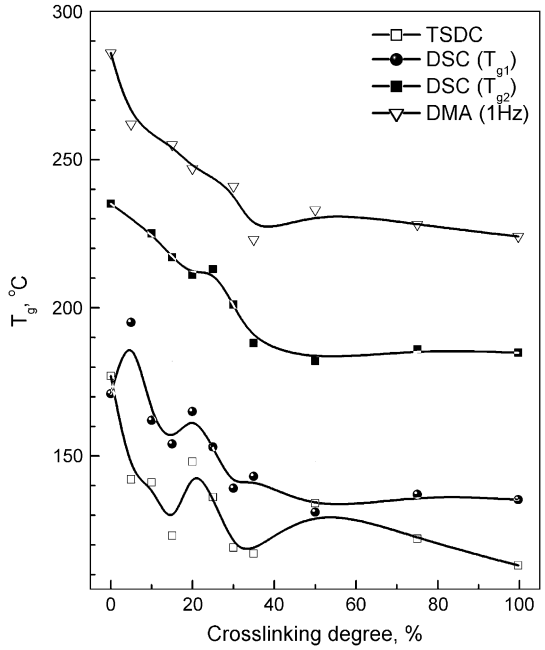

Fig. 8. T_g versus crosslinking degree dependencies obtained for the whole series of HBPIs as estimated by three different techniques.

where the equivalent frequencies were ca. 10^{-2} and 10^{-4} Hz, respectively. Besides, it may be supposed that the absence of the second, higher-temperature TSDC peak is explained with its masking by conductivity. Nevertheless, these reasons cannot be responsible for 100 °C difference in T_g values or, especially, manifestation of two- or three-stage glass transition.

The globular HBPI structure prevents chain entanglement; it is possible for these macromolecules to aggregate together due to intermolecular interaction forces, such as hydrogen bonds, and some interpenetration of the surface branches of neighboring hyperbranched molecules. We believe that the peculiar, complicated glass transition dynamics in the HBPIs may be treated tentatively in terms of structural/dynamic nanoheterogeneity, different dynamics of exterior and interior domains in HBPI molecular nanoglobules (*inter-* or *intraglobular* dynamics), and loosening their packing with increase in free volume at EGDE crosslinking, especially at small or moderate crosslinking densities. Just the absence of well-defined molecular architecture of HBPIs and presumably different dynamics of interior and exterior regions of their nanoglobules (see a scheme in Fig. 1) may result, indeed, in very broad glass transition with its two-stage manifestation.

As for the effect of crosslinking with EGDE, two points must be taken *a priori* into account:

(a) HBPI molecular structure is modified by introducing EGDE "bridges";
(b) EGDE molecules may apparently penetrate, to some extent, into HBPAA globules in solution, however, the crosslinking reaction sites must be located predominantly in the exterior regions of globular hyperbranched macromolecules.

Table 1
Comparative transport parameters for air gases in polymeric membranes based on hyperbranched and linear polyimides

Polymer	P_{N_2} (Barrer)	P_{O_2} (Barrer)	P_{CO_2} (Barrer)	$\alpha = P_{N_2}/P_{O_2}$
Linear PMDA–ODA polyimide	0.05	0.05	1.14	1.0
Hyperbranched ODPA–TAP polyimide	0.8	0.42	0.28	1.9
HBPI crosslinked by 20% with EGDE	4.4	2.44	1.42	1.8
HBPI crosslinked by 35% with EGDE	8.5	1.35	2.93	6.3

Notes: 1. P and α are permeability coefficient and selectivity, respectively.
2. The accuracy of measurements was ±10%.

In our opinion, EGDE ''bridges'' cannot apparently be considered as a real plasticizer since these molecules are rigidly (covalently) attached from both ends to HBPI globules, and EGDE molecular length does not exceed typical Kuhn segment size in flexible-chain molecules (~1.5–2.0 nm) [42]. This means that segmental dynamics within EGDE linkage is to be forbidden.

On the other hand, the larger changes with crosslinking may presumably be expected for the interglobular dynamics, due to facilitated accession of exterior domains in HBPI globules to EGDE; moving the globules apart; loosening interglobular packing with increasing free volume resulting in better permeability (see Table 1 and a scheme in Fig. 1). We suppose that the decrease of T_g with crosslinking HBPIs up to c.d. = 35% was caused just by this reason. Actually, Fig. 4a indicates larger decrease of T_{g2} with crosslinking, as compared to T_{g1}. Besides, Fig. 4b shows that the intensity of DSC glass transition 1 remained nearly invariable after crosslinking, whereas the intensity of glass transition 2 increased twice. This allowed us to tentatively assign glass transitions 1 and 2 to ''unfreezing'' intra- or interglobular dynamics, respectively.

Thus, unlike DSC and CRS techniques which distinctly revealed dynamic heterogeneity in HBPI glass transition, TSDC thermograms permitted to observe only intraglobular dynamics. Meantime, the relative closeness, by taking into account of the difference in time experimental conditions, of T_{g2} (DSC) and DMA peak location may testify in favor of the main role of interglobular dynamics in formation of the mechanical loss spectrum.

Preliminary comparative estimation of transport properties for N_2, O_2 and CO_2 of membranes, prepared from the HBPIs studied and linear PI, was made. Besides the crosslinked HBPI films with the improved mechanical properties, it was useful also to compare these films with the uncrosslinked, starting HBPI film. Under certain conditions of careful treatment of this film, it was possible to prepare self-standing film, with a poor mechanical quality, and to use it for permeability analyses.

The permeability coefficients P and selectivities α for some membranes are given in Table 1. One can see that these data are consistent with the conclusion about increasing free volume in HBPIs, especially after their crosslinking with EGDE. Actually, permeability coefficients for N_2 and O_2 are much higher in HBPI than for linear PI. Besides, unlike the usual decrease in gas permeability with an increase in crosslinking degree, as it is typically observed for linear polymers, crosslinking HBPI resulted in increased permeability coefficients, e.g., for N_2 and CO_2, by one order of magnitude; selectivity $\alpha(N_2/O_2)$ also increased. Thus, on the whole the transport of gas molecules through HBPI became easier after its crosslinking due to loosened packing of nanoglobules.

4. Conclusion

Combined DSC/TSDC/DMA/CRS dynamic analysis at 20–300 °C was performed for a series of EGDE-crosslinked hyperbranched ODPA–TAP polyimides with regularly varied crosslinking density. It was revealed that the complex molecular structure of the HBPIs resulted in manifestation of a peculiar glass transition dynamics in these systems. Two- or three-stage transitions over very broad temperature range, and a substantial decrease of T_gs with an increase in crosslinking density of HBPI nanoglobules, were shown. Manifestation of the glass transition depended on the measuring technique used: different displaying transition dynamics in heat capacity, discharging current, mechanical losses or creep rate measurements were observed. Thus, unlike the lower- and higher-temperature glass transition stages found out by DSC, only the former stage was observed in the TSDC thermograms but basically the latter stage was strongly pronounced when using the mechanical relaxation spectrometry techniques (DMA, CRS). Such special dynamic behavior was treated tentatively in terms of dynamic nanoheterogeneity with separate manifesting *intra-* and *interglobular* dynamics in HBPIs, and of loosening molecular packing due to crosslinking with EGDE. Considerably increased air gas permeability and selectivity of the EGDE-crosslinked, self-standing HBPI films as compared with those for linear polyimide, were evidenced.

Acknowledgements

This work was supported by the Grant Agency of the Czech Republic (Grant No. 203/06/1086) and also co-funded by the European Social Fund and Greek National Resources-PYTHAGORAS-II.

References

[1] Jikei M, Kakimoto M. J Polym Sci Part A Polym Chem 2004;42(6):1293–309.
[2] Jikei M, Kakimoto M. Progr Polym Sci 2001;26(8):1233–85.
[3] Gao C, Yan D. Progr Polym Sci 2004;29(3):149–82.
[4] Ohya H, Kudryavtsev VV, Semenova SI. Polyimide membranes – applications, fabrication and properties. Tokyo: Gordon and Breach Publishers; 1996.
[5] Schauer J, Sysel P, Marousek V, Pientka Z, Pokorny J, Bleha M. J Appl Polym Sci 1996;61:1333–7.
[6] Fang J, Kita H, Okamoto K. J Membr Sci 2001;182:245–56.
[7] Sindelar V, Sysel P, Hynek V, Friess K, Sipek M, Castaneda N. Collect Czech Chem Commun 2001;66:533–8.
[8] Kim YH. J Polym Sci Part A Polym Chem 1998;36:1685.
[9] Fang J, Kita H, Okamoto K. Macromolecules 2000;33:4639–46.

[10] Yamanaka K, Jikei M, Kakimoto M. Macromolecules 2000;33(4):1111–4.
[11] Yamanaka K, Jikei M, Kakimoto M, Nihira T, Nakayama T. J Photopolym Sci Technol 2000;13(2):321–2.
[12] Yamanaka K, Jikei M, Kakimoto M. Macromolecules 2000;33(19):6937–44.
[13] Yamanaka K, Jikei M, Kakimoto M. J Photopolym Sci Technol 2001;14(1):11–6.
[14] Yamanaka K, Jikei M, Kakimoto M. Macromolecules 2001;34(12):3910–5.
[15] Chen H, Yin J. J Polym Sci Part A Polym Chem 2002;40(21):3804–14.
[16] Makita S, Kudo H, Nishikubo T. J Photopolym Sci Technol 2002;15(2):185–9.
[17] Hao J, Jikei M, Kakimoto M. Macromol Symp 2003;199:233–41.
[18] Chen H, Yin J. Polym Bull 2003;50(5–6):303–10.
[19] Chen H, Yin J. J Polym Sci Part A Polym Chem 2003;41(13):2026–35.
[20] Wang KL, Jikei M, Kakimoto M. J Photopolym Sci Technol 2003;16(2):267–8.
[21] Chen H, Yin J, Xu H. Polym J 2003;35(3):280–5.
[22] Chen H, Yin J. Polym Bull 2003;49(5):313–20.
[23] Liu C, Naismith N, Huang Y, Economy J. J Polym Sci Part A Polym Chem 2003;41(23):3736–43.
[24] Wang KL, Jikei M, Kakimoto M. J Polym Sci Part A Polym Chem 2004;42(13):3200–11.
[25] Suzuki T, Yamada Y. J Polym Sci Part B Polym Phys 2006;44(2):291–8.
[26] Ekinci E, Emre FB, Koytepe S, Secëkin T. J Polym Res 2005;12(3):205–10.
[27] Suzuki T, Yamada Y. Polym Bull 2005;53(2):139–46.
[28] Koytepe S, Pasëahan A, Ekinci E, Secëkin T. Eur Polym J 2005;41(1):121–7.
[29] Suzuki T, Yamada Y, Tsujita Y. Polymer 2004;45(21):7167–71.
[30] Makita S, Kudo H, Nishikubo T. J Polym Sci Part A Polym Chem 2004;42(15):3697–707.
[31] Chen H, Yin J. J Polym Sci Part A Polym Chem 2004;42(7):1735–44.
[32] Yin Y, Yang L, Yoshino M, Fang J, Tanaka K, Kita H, et al. Polym J 2004;36(4):294–302.
[33] Hao J, Jikei M, Kakimoto M. Macromolecules 2003;36:3519–25.
[34] Jikei M, Kakimoto M. J Polym Sci Part A Polym Chem 2004;42:1293–309.
[35] Liu Y, Chung T. J Polym Sci Part A Polym Chem 2002;40:4563–9.
[36] Sysel P, Kotek J, Peter J, Hobzova R, Snablova-Frycova M, Hynek V, et al. Plasty a Kaucuk 2005;42(5–6):6–12.
[37] Van Turnhout J. In: Sessler GM, editor. Topics in applied physics, vol. 33. Berlin: Springer; 1980. p. 81–215.
[38] Peschanskaya NN, Yakushev PN, Sinani AB, Bershtein VA. Thermochim Acta 1994;238:429–52.
[39] Peschanskaya NN, Yakushev PN, Sinani AB, Bershtein VA. Macromol Symp 1997;119:79–87.
[40] Bershtein VA, Yakushev PN, Peschanskaya NN. Macromol Symp 1999;147:73–80.
[41] Bershtein VA, David L, Egorov VM, Pissis P, Sysel P, Yakushev PN. In: Mittal KL, editor. Polyimides and other high temperature polymers, vol. 3. Utrecht–Boston: VSP; 2005. p. 353–99.
[42] Bershtein VA, Egorov VM. Differential scanning calorimetry of polymers. Physics, chemistry, analysis, technology. New York: Ellis Horwood; 1994.